Joseph George[a,*]

Determination of selenium during pathogenesis of hepatic fibrosis employing hydride generation and inductively coupled plasma mass spectrometry

https://doi.org/10.1515/hsz-2017-0260
Received October 4, 2017; accepted January 11, 2018; previously published online February 6, 2018

Abstract: Serum and liver selenium levels were studied during the pathogenesis of *N*-nitrosodimethylamine (NDMA) induced hepatic fibrosis in rats. The degree of fibrosis was assessed with Masson's trichrome staining and quantifying collagen content in the liver. Lipid peroxides were measured in blood and liver samples and total glutathione and glutathione peroxidase were assayed in the liver tissue to evaluate oxidative stress. Interleukin-6 (IL-6) and transforming growth factor-β1 (TGF-β1) were measured in the serum. Selenium levels were determined using inductively coupled plasma-mass spectrometry (ICP-MS) after acid digestion and hydride generation of selenium. Serial administrations of NDMA produced well-developed fibrosis and early cirrhosis in the liver with 4-fold increase of total collagen content and deposition of collagen fibers. Blood and hepatic lipid peroxides, serum IL-6 and TGF-β1 were significantly increased. There was significant reduction in hepatic glutathione and glutathione peroxidase levels. Serum and liver selenium were remarkably decreased on all the days studied. The results suggest that decreased selenium and glutathione peroxidase contribute to the impairment of cellular antioxidant defense, which in turn results in oxidative stress and trigger pathogenesis of hepatic fibrosis. The study further demonstrated that ICP-MS with hydride generation technique is a reliable and sensitive method for determination of selenium in biological samples.

Keywords: dimethylnitrosamine; glutathione peroxidase; hepatic fibrosis; ICP-MS; *N*-nitrosodimethylamine; selenium.

[a]Department of Biochemistry, Central Leather Research Institute, Adyar, Madras 600 020, India
***Corresponding author (Present address): Joseph George,** Department of Hepatology, Kanazawa Medical University, 1-1 Daigaku, Uchinada, Ishikawa 920-0293, Japan,
e-mail: georgej@kanazawa-med.ac.jp.
http://orcid.org/0000-0001-5354-7884

Introduction

Hepatic fibrosis is the result of continuous wound healing response to a variety of chronic stimuli, such as ethanol, viral infection, toxins, or cholestasis (Mormone et al., 2011; Zhang et al., 2016). Excessive deposition of collagens and other connective tissue components in the liver is the hallmark of hepatic fibrosis (George et al., 2001, 2017). Despite enormous advancement in the field, the precise mechanism involved in the pathogenesis and progression of hepatic fibrosis is not clear. The chronic stimuli involved in the initiation of fibrosis leads to oxidative stress and generation of reactive oxygen species (ROS) that serve as mediators of molecular events involved in liver fibrosis (Sánchez-Valle et al., 2012). These processes lead to cellular injury and trigger inflammatory responses releasing a variety of cytokines that stimulate synthesis of excessive connective tissue components results in fibrosis (Alegre et al., 2017).

Selenium is an essential trace element and an integral component of glutathione peroxidase, an enzyme that protects cellular membrane damage from lipid peroxidation. Selenium is also considered as an anticancer agent that prevents the processes of cell proliferation and tumor growth (Brenneisen et al., 2005). It was reported that serum selenium level is strongly associated with the severity of liver damage (Petrovski et al., 2012). A diminished anti-oxidant status and decreased serum selenium levels were observed in patients with alcoholic liver cirrhosis (Korpela et al., 1985; Burk et al., 1998; Rua et al., 2014). It was suggested that decreased serum selenium levels might play a role in the pathogenesis and progression of alcoholic liver disease (Prystupa et al., 2017). However, the pathophysiological correlation of selenium deficiency and progression of liver diseases is not clear and could be attributed to glutathione peroxidase and oxidative stress.

Even though several investigators have reported serum selenium levels in experimentally induced hepatic fibrosis and in patients with alcoholic liver cirrhosis, the data are highly variable, probably due to different and insensitive methods employed for the determination of selenium.

Besides, data are not available regarding alteration of liver selenium levels during pathogenesis of hepatic fibrosis. As selenium is involved in the antioxidant defense of liver tissue, selenium levels in the liver are more important compared to serum levels. The current study was aimed to determine both serum and liver selenium levels using a very sensitive and specific method employing inductively coupled plasma-mass spectrometry (ICP-MS) after acid extraction and hydride generation of selenium. The study further aimed to determine the correlation between selenium concentration and pro-fibrotic cytokines during the pathogenesis of experimentally induced hepatic fibrosis.

Results

Alteration of animal body weight and liver weight

The alteration of animal body weight and liver weight during the course of N-nitrosodimethylamine (NDMA) administration is presented in Figure 1A. There was significant decrease in animal body weight on day 14 ($p < 0.01$) and day 21 ($p < 0.001$) following NDMA administration. The liver weight was also reduced significantly ($p < 0.001$) on days 14 and 21. A slight increase was noticed in the mean liver weight on day 7, but the difference was not significant.

Assessment of the degree of NDMA-induced hepatic fibrosis

The degree of NDMA-induced hepatic fibrosis was assessed both biochemically and histologically. The total collagen content in the liver tissue increased significantly ($p < 0.001$) on 7th, 14th and 21st days following NDMA administration (Figure 1B). A maximum increase of 4-fold was noticed on day 21 compared to the untreated controls.

Histologically, untreated control rat livers depicted normal lobular architecture with central veins and radiating hepatic cords (Figure 2A). On day 7, centrilobular hepatocyte necrosis and focal hemorrhage was present. There was significant dilatation of central veins and sinusoids and initiation of fibrosis (Figure 2B). On day 14, marked fibrosis with deposition of collagen fibers was conspicuous (Figure 2C). Hemorrhagic necrosis and apoptosis of hepatocytes were also present. On day 21, well-developed fibrosis and early cirrhosis with thick collagen fibers were prominently present (Figure 2D).

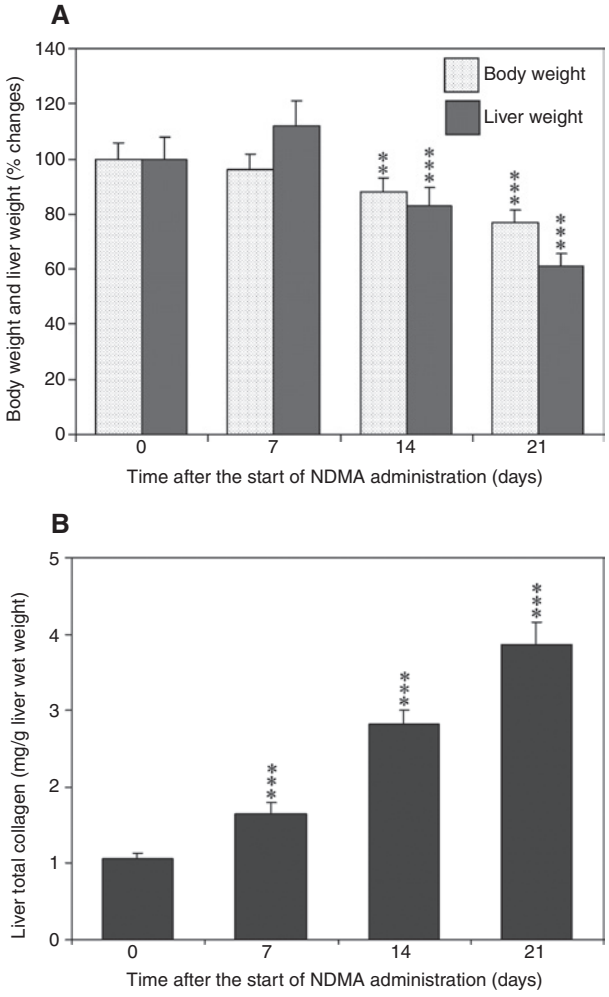

Figure 1: Alteration of animal body weight, liver weight, and liver collagen content during pathogenesis of hepatic fibrosis.
(A) Changes in body weight and liver weight following NDMA administration. The data are mean ± SD of 12 rats per group. $^{**}p < 0.01$ and $^{***}p < 0.001$ NDMA-treated rats vs. untreated control rats. (B) Increase of total collagen content in the liver after the start of NDMA administration. The data are mean ± SD of 12 animals per group. $^{***}p < 0.001$ NDMA-treated rats vs. untreated control rats.

There was hemorrhagic necrosis and regeneration of hepatocytes.

Masson's trichrome staining for mature collagen is presented in Figure 3. Staining for collagen was absent in untreated control livers except in central veins (Figure 3A). On day 7, fibrosis was initiated with the deposition of collagen fibers between central vein and portal tracts (Figure 3B). On day 14, intermittent deposition of thick collagen fibers was present in the liver parenchyma (arrows) (Figure 3C). On day 21, there was extensive deposition of thick collagen fibers between central vein and portal tracts that formed well-developed bridging fibrosis and early cirrhosis (Figure 3D).

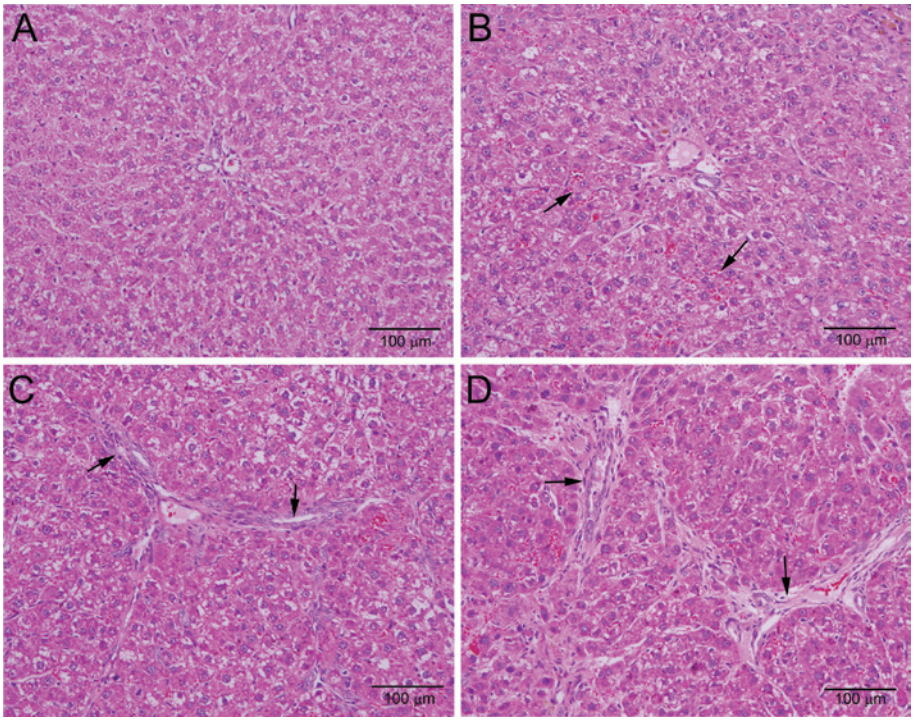

Figure 2: Hematoxylin and eosin (H&E) staining of rat liver sections following NDMA administration.
(A) Normal liver. (B) Day 7. Dilation of sinusoids with focal hemorrhage (arrows). Centrilobular hepatocyte necrosis and initiation of fibrosis. (C) Day 14. Focal hemorrhagic necrosis. Formation of fibrosis and deposition of collagen fibers (arrows). (D) Day 21. Well-developed fibrosis and early cirrhosis with thick collagen fibers (arrows). Original magnification, ×100.

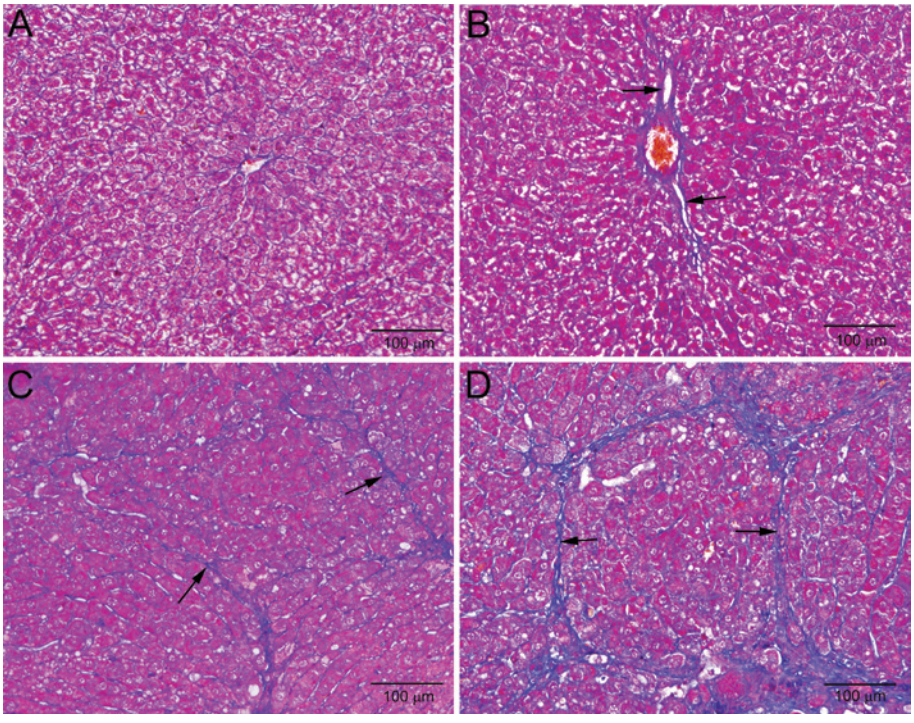

Figure 3: Masson's trichrome staining for collagen in rat liver sections following NDMA administration.
(A) Normal liver. (B) Day 7. Initiation of fibrosis and beginning of deposition of collagen fibers (arrows). (C) Day 14. Development of fibrosis and deposition of collagen fibers (arrows). (D) Day 21. Marked hepatic fibrosis and early cirrhosis. Accumulation of extensive collagen fibers in the liver parenchyma (arrows). Original magnification, ×100.

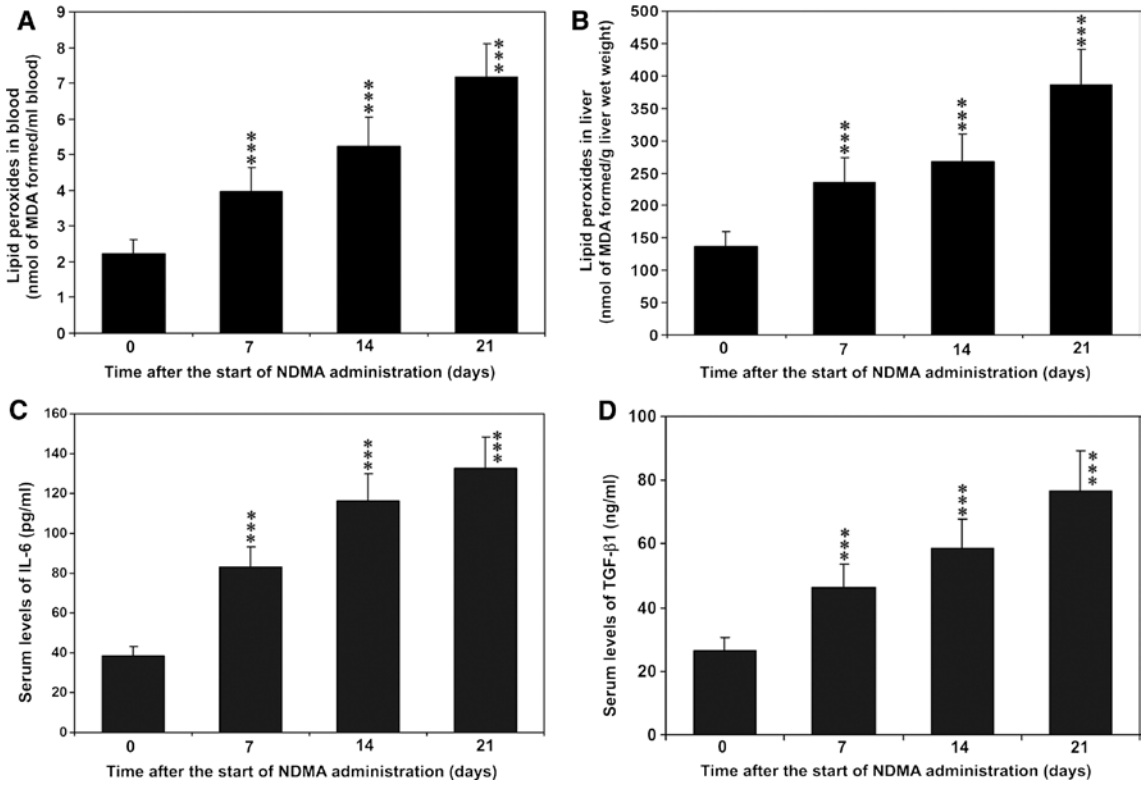

Figure 4: Lipid peroxides in the blood (A) and liver (B) during the progression of NDMA-induced hepatic fibrosis in rats. Lipid peroxides present in both blood and liver tissue were markedly elevated on 7th, 14th and 21st days following NDMA administration. The lipid peroxides are expressed as nanomoles of malondialdehyde (MDA) formed. Serum levels of IL-6 (C) and TGF-β1 (D) during the pathogenesis of NDMA-induced hepatic fibrosis in rats. Both IL-6 and TGF-β1 increased significantly on 7th, 14th and 21st days following NDMA administration. All data are mean ± SD of 12 animals per group. ***$p < 0.001$ NDMA-treated vs. untreated control rats.

Increased oxidative stress and elevation of lipid peroxides

Lipid peroxides in blood and liver tissue measured in terms of malondialdehyde formed is presented in Figure 4A and B, respectively. Lipid peroxides were significantly increased ($p < 0.001$) on 7th, 14th and 21st days in both blood and liver tissue following NDMA administration. The increase was gradual and the maximum increase was observed on day 21 in both blood and liver samples. There was a positive correlation (r = 0.992) between increased lipid peroxides in blood and liver tissue.

NDMA administration increased IL-6 and TGF-β1 in rat serum

Interleukin-6 (IL-6) is a pro-inflammatory cytokine. Serum IL-6 levels significantly increased ($p < 0.001$) on 7th, 14th and 21st days following NDMA administration (Figure 4C). As in the case of IL-6, serum transforming growth factor-β1 (TGF-β1) level also increased significantly ($p < 0.001$) on all the days measured following NDMA administration (Figure 4D). The maximum increase was observed on day 21, which was around 3-fold compared to the mean serum TGF-β1 levels in untreated control rats.

Marked decrease of glutathione and glutathione peroxidase in rat liver

The total glutathione levels (GSH + GSSG) and glutathione peroxidase activity in the liver homogenate are presented in Figure 5A and B, respectively. Both glutathione levels and glutathione peroxidase activity were significantly decreased ($p < 0.001$) on 7th, 14th and 21st days following administration of NDMA. The decrease was gradual and the maximum decrease was observed on day 21 for both glutathione and glutathione peroxidase. A positive correlation (r = 0.993) was present between decreased glutathione levels and glutathione peroxidase activity. Similarly, a strong negative correlation (r = – 0.989) was observed between elevated lipid peroxides in the liver and decreased glutathione levels.

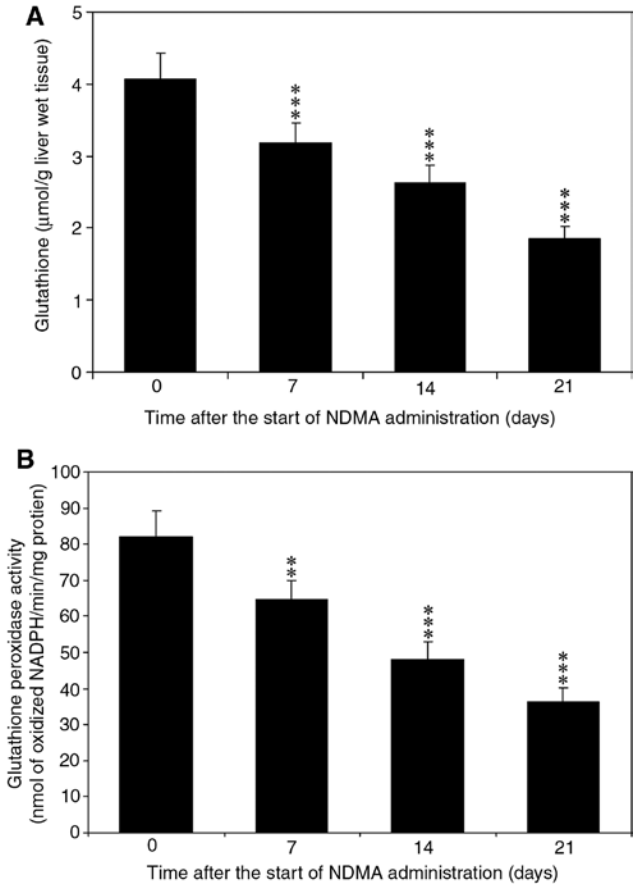

Figure 5: Glutathione and glutathione peroxidase in rat liver during pathogenesis of hepatic fibrosis.
(A) Decreased total glutathione (GSH + GSSG) levels in rat liver following NDMA administration and (B) glutathione peroxidase activity in rat liver. There was a significant decrease in glutathione peroxidase activity in the liver tissue of rats during pathogenesis of NDMA-induced hepatic fibrosis. The data are mean ± SD of 12 animals per group. ***$p < 0.001$ NDMA-treated vs. untreated control rats.

Significant decrease of selenium levels in serum and liver

Selenium levels in the serum and liver tissue are presented in Figure 6. Serum selenium levels decreased significantly ($p < 0.001$) on all the days studied during the pathogenesis of NDMA-induced hepatic fibrosis (Figure 6A). The decrease was gradual and the maximum decrease (around 2.5-fold) was observed on day 21 compared to the serum selenium levels in untreated control rats. The liver selenium levels were also decreased significantly ($p < 0.001$) on 7th, 14th and 21st days following NDMA administration (Figure 6B). The maximum decrease was observed on day 21, which was around 2.3-fold compared to the untreated controls. A positive correlation (r = 0.981) was observed between decreased serum and liver selenium levels. Similarly, there was also a positive correlation (r = 0.966) between reduced glutathione peroxidase levels and decreased selenium levels in the liver.

Rate of recovery of selenium in reference samples

The results of spike and recovery of selenium in reference samples are presented in Table 1. Two known concentration of selenium was added to both serum samples and liver extract within the assay range and processed along with the samples without the addition of spike in control. The results depicted a recovery rate between 97 and 104% in the spiked reference samples. The data indicate that the ICP-MS with hydride generation technique is a sensitive and reliable method for determination of selenium in biological samples compared to the other existing methods.

Discussion

In the current study, we developed a very sensitive and reliable method for determination of selenium in biological samples. In the conventional direct nebulization method, detection limit of selenium is relatively poor in serum and tissue samples and the selenium, which is covalently linked to vital enzymes such as glutathione peroxidase, may not be detected completely. Hydride generation is a very effective analytical technique to separate hydride forming metals such as selenium from a range of matrices and varying acid concentrations.

The serum and liver selenium levels obtained in the present study are significantly higher compared to the values reported earlier (Laclaustra et al., 2009; Lu et al., 2016; Ojeda et al., 2017). Here, we employed a specific protocol and technique of acid digestion and hydride generation for better analytical sensitivity. In this technique, selenium is vaporized, atomized and ionized and the ions are detected a by mass spectrometer, which is an ultralow level detection method for trace elements (Khan et al., 2014). Due to its very high sensitivity and specificity to detect ultralow levels of selenium, it is almost certain that the entire selenium present in the samples were detected, which could be the reason for higher selenium content compared to other investigators.

In a recent publication, the mean value of selenium reported in normal rat serum was 205.35 ± 6.86 µg/l and in rat liver, it was 200 ± 12 ng/g dry weight (Ojeda et al., 2017). In the current study, it was 518.7 ± 28.5 µg/l and 653.2 ± 36.8 ng/g wet weight, respectively, which are almost 3-fold

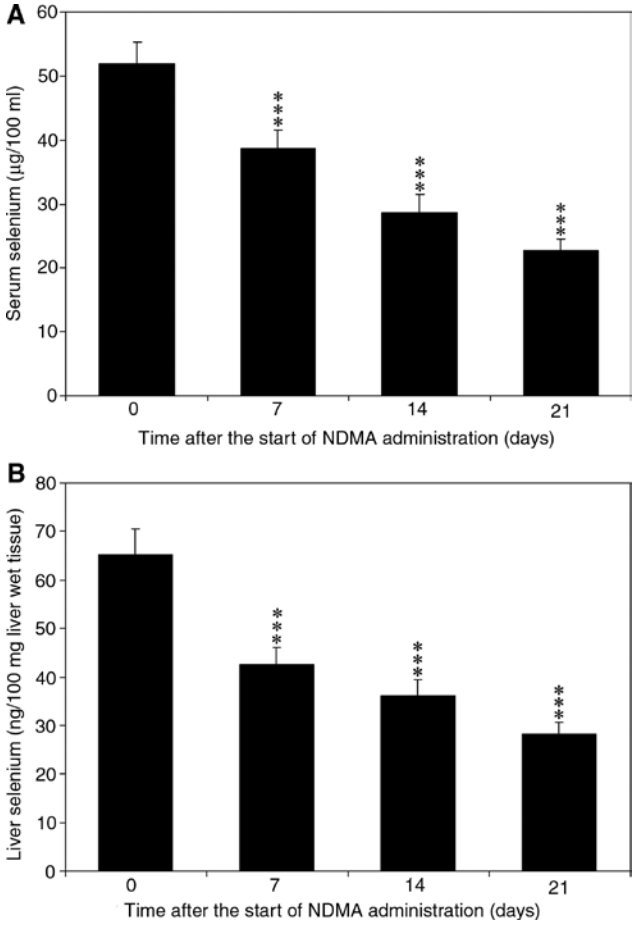

Figure 6: Selenium levels in serum (A) and liver (B) during the pathogenesis of NDMA-induced hepatic fibrosis in rats. Selenium levels in both serum and liver were significantly ($p < 0.001$) decreased on 7th, 14th and 21st days following NDMA administration. The data are mean ± SD of 12 animals per group. ***$p < 0.001$ NDMA-treated vs. untreated control rats.

higher compared to the values in the above study. The authors used graphite-furnace atomic absorption spectrometry for determination of selenium, which is a much less sensitive technique compared to the ICP-MS method used in the present study. Moreover, they did not use hydride generation technique, which enables complete detection of intracellular and protein bound selenium in biological samples. In another study, the authors used single-tube fluorimetric assay to determine selenium levels in human serum and they obtained a mean value of 100.6 µg/l (Pemberton et al., 2005). Another group determined selenium levels in healthy human blood samples using inductively coupled plasma atomic emission spectroscopy (ICP-AES) without hydride generation technique and obtained a mean value of 187 ± 4.4 ng/l (Massadeh et al., 2010). In ICP-AES, the excited atoms and ions that emit electromagnetic radiation at a particular wavelength characteristic of an element is detected on a spectrometer. In a mass spectrometer, the excited ions are detected based on the mass of a particular element, where the technique has better sensitivity and specificity compared to AES. Even though, ICP-AES is less sensitive and specific compared to ICP-MS for detection of selenium in biological samples, ICP-AES is considered as one of the reliable and easy methods for detection of large number of elements.

Increased oxidative stress and lipid peroxidation is a common feature in experimentally induced hepatic fibrosis (George, 2008; Gutiérrez et al., 2010). Extensive oxidative stress and production of ROS trigger collagen synthetic machinery that culminates in well-developed fibrosis and cirrhosis (Richter and Kietzmann, 2016). In the present study, lipid peroxides were increased markedly in both blood and liver samples following treatment with NDMA. In healthy liver, the presence of a strong multifaceted antioxidant system instantly destroys excessive production of free radicals and ROS, which prevents increase of oxidative stress. However, during NDMA administration the balance between 'generation and destruction' of free radicals and ROS is impaired due to extensive production of ROS and decreased antioxidant system. The positive correlation observed between increased lipid peroxides in the blood and liver samples indicates extra-hepatic circulation of lipid peroxides generated in the liver. The extensive centrilobular necrosis of the liver during NDMA administration could answer for the elevation of lipid peroxides in circulation.

Interleukin-6 is a pro-inflammatory cytokine secreted by T-cells and macrophages during infection and trauma

Table 1: Spike and recovery of selenium in serum samples and liver extract employing inductively coupled plasma-mass spectrometry after acid digestion and hydride generation of selenium.

Sample (n = 6)	Spike level	Observed range (ng)	Mean (ng)	Recovery (%)
Serum	500 ng/ml	483–516	495	99
Serum	1000 ng/ml	965–1021	983	98
Liver extract	50 ng/100 mg	46–55	52	104
Liver extract	100 ng/100 mg	92–106	97	97

The samples were assayed after adding respective concentration of selenium spike stock solution. Values reported for spiked samples reflect subtraction of the endogenous selenium present in the samples. The mean represents the average of six samples.

leading to inflammation. IL-6 plays a significant role in the pathogenesis of hepatic fibrosis and regeneration of the damaged liver (Schmidt-Arras and Rose-John, 2016). In the present study, serial administrations of NDMA over a period of 3 weeks produce extreme necrosis and inflammation in the liver, which resulted in a significant elevation of IL-6 in serum. Increased serum IL-6 has also been reported in carbon tetrachloride-induced hepatic fibrosis (Lin et al., 2015). The role of TGF-β1 in molecular pathogenesis of hepatic fibrosis has been studied extensively and is considered as the most potent fibrogenic cytokine (Seki and Brenner, 2015). TGF-β increases ROS production and decreases the concentration of glutathione, which mediates many of the fibrogenic effects of TGF-β in various types of cells (Liu and Gaston Pravia, 2010). In the current study also, there was marked elevation of TGF-β1 that contributed to the pathogenesis of NDMA-induced hepatic fibrosis.

Glutathione is responsible for the protection of cells from free radical mediated damages and serves as a cofactor for a number of antioxidant and detoxifying enzymes (Ribas et al., 2014). Glutathione is a tripeptide comprising three amino acids (cysteine, glutamic acid and glycine) and 90–95% of the total glutathione is present in reduced form (GSH). Oxidation of glutathione leads to the formation of glutathione disulfide (GSSG). When cells are exposed to increased levels of oxidative stress, GSSG accumulates in the cell and the ratio of GSSG to GSH increases. Glutathione peroxidase (GPx) converts reduced glutathione (GSH) to oxidized form (GSSG), while reducing lipid hydroperoxides to their corresponding alcohols or free hydrogen peroxide to water. Glutathione peroxidase comprises a family of eight isoenzymes that are encoded by different genes and not all of them are selenoproteins (Brigelius-Flohé and Maiorino, 2013). GPx1 is selenium-dependant and the most abundant GPx isoenzyme present in the cytoplasm of mammalian tissues that reduces hydrogen peroxide to water (Lubos et al., 2011). Glutathione reductase catalyzes the reduction of oxidized glutathione to its reduced form. The marked decrease of cellular glutathione and GPx activity observed in the present study indicates that the impaired antioxidant status of hepatocytes significantly contributes towards the pathogenesis of NDMA induced hepatic fibrosis. This is further corroborates with a remarkable decrease of both blood and liver ascorbic acid levels noticed in our previous study (George, 2003).

Selenium is an integral component of GPx and thus plays an important role in cellular antioxidant system (Tinggi, 2008). Decreased levels of serum selenium have been reported in alcoholic liver diseases (Korpela et al., 1985; Burk et al., 1998; González-Reimers et al., 2008; Rua et al., 2014). Reduced hepatic selenium has been observed in experimental binge drinking (13) and patients with alcoholic cirrhosis (Thuluvath and Triger, 1992; Dworkin et al., 1988). In the current study, a marked decrease was observed in both serum and liver selenium levels following NDMA administration. It was postulated that the depleted serum selenium concentration in liver cirrhosis is due to the consequence of a liver dysfunction (Valimaki et al., 1983). As selenium is a trace element mostly linked to antioxidant enzymes, the depleted selenium levels in both serum and liver tissue during experimental hepatic fibrosis and alcoholic liver diseases could be attributed to a marked decrease of antioxidant status. It is important to note that selenium is an integral part of GPx and other selenoproteins and selenoenzymes that are mainly involved in the defense mechanism for oxidative stress.

The data of the present study strongly suggest that there is a correlation between rise in lipid peroxides, elevated levels of IL-6 and TGF-β1, marked decrease of hepatic GSH and GPx, and decreased levels of serum and hepatic selenium, which altogether significantly contribute to the pathogenesis NDMA-induced hepatic fibrosis. A positive correlation with markers of fibrosis and decreased serum selenium has been implicated in liver cirrhosis (Casaril et al., 1989). Selenium functions as a dietary antioxidant and decreased levels of selenium play a probable role in the pathogenesis of several chronic diseases (Boosalis, 2008). Taken together, our study indicates that the marked decrease of antioxidant status in liver disease is responsible for decreased selenium levels, which in turn contribute to the pathogenesis of hepatic fibrosis.

In conclusion, the results of the present study demonstrated that there is a significant decrease of selenium in both serum and liver during pathogenesis and progression of hepatic fibrosis. The decreased selenium could be correlated with reduced glutathione peroxidase levels and may contribute to the impairment of cellular antioxidant defense, which in turn results in oxidative stress and trigger pathogenesis of hepatic fibrosis. The study further demonstrated that ICP-MS with hydride generation technique is a very sensitive and reliable method for determination of selenium in biological samples.

Materials and methods

Animals

Wistar adult male albino rats at the age of 3 months were used in the experiment. Three-month-old male rats were selected for the study as they are young adults without diseases and could produce uniform fibrosis (George et al., 2001). All the animals received humane

care and maintained under 12-h light/12-h dark cycles in an air-conditioned animal house, with commercial rat feed pellets (Hindustan Lever, Bombay, India) and water available *ad libitum*. This is a standard animal feed and does not contain any extra amount of selenium. The animal experiments were carried out with following the Guide for the Care and Use of Laboratory Animals, prepared by the National Academy of Sciences and published by the US National Institutes of Health (NIH Publication No. 86-23, revised 1996). The experimental protocol was approved by the Institutional Animal Care and Use Committee (IACUC).

Induction of hepatic fibrosis

Hepatic fibrosis was induced by serial intraperitoneal injections of NDMA (Sigma-Aldrich, St. Louis, MO, USA) in doses of 1 mg (10 µl diluted to 1 ml with 0.15 mol/l sterile NaCl)/100 g body weight on three consecutive days of every week over a period of 21 days (George et al., 2001). Control groups received similar injections without NDMA. Animals' body weight and behavioral changes were monitored throughout the study. The animals were sacrificed on days 7, 14 and 21 from the beginning of exposure. Blood was collected from the right jugular vein under anesthesia with diethyl ether and the serum was stored at −80°C until assayed. The liver was rapidly removed, washed in cold phosphate buffered saline, and weighed in the wet state after blotting off water. A median lobe of 3 mm thick was cut and instantly fixed in 10% phosphate-buffered formalin for histopathological studies. Another portion of the liver was frozen at −80°C for biochemical studies.

Histopathological evaluation of NDMA-induced hepatic fibrosis

The degree of NDMA-induced hepatic fibrosis was evaluated histopathologically after hematoxylin and eosin (H&E) and Masson's trichrome staining employing conventional protocols. The stained sections were examined with an Olympus BX51 microscope (Olympus, Tokyo, Japan) and photographed.

Estimation of hydroxyproline and collagen content in the liver

Hydroxyproline levels and total collagen content in the liver tissue were determined for the biochemical evaluation of the degree of hepatic fibrosis after treatment with NDMA. Hydroxyproline content in the liver tissue was determined as described before (Jamall et al., 1981) using *L*-hydroxyproline (Sigma-Aldrich, St. Louis, MO, USA) as a standard. The total collagen content in the liver tissue was calculated by multiplying the hydroxyproline content by the factor 7.46 as described previously (George and Chandrakasan, 1996).

Measurement of lipid peroxides in blood and liver tissue

The lipid peroxides present in the blood sample were determined using the spectrofluorometric method as described before (George, 2003). Lipid peroxides present in the liver tissue were measured employing thiobarbituric acid reaction (Gheita and Kenawy, 2014) using tetramethoxypropane (Sigma-Aldrich, St. Louis, MO, USA) as standard and the data are presented as nmoles malondialdehyde formed/g liver wet weight.

Measurement of interleukin-6 and TGF-β1 in rat serum

The serum samples were analyzed for IL-6 (Cat #ab100772) and TGF-β1 (Cat #ab119558) using ELISA kits from Abcam (Cambridge, MA, USA) as per the manufacturer's protocol. The absorbance of the final reaction product was measured on a microplate plate reader (BioRad, Hercules, CA, USA) at 450 nm.

Measurement of glutathione and glutathione peroxidase in the liver

Total glutathione (GSH + GSSG) present in the liver homogenate was determined using a glutathione assay kit (Cat #CS0260, Sigma-Aldrich, St. Louis, MO, USA). Exactly 100 mg of frozen liver tissue was homogenized in 1 ml of ice cold 50 mM Tris-HCl buffer (pH 8) containing 150 mM NaCl, 1 mM EDTA, and 1% Triton X-100 and used for the glutathione assay. The total glutathione content in the liver is presented as µmoles/g fresh liver tissue.

Glutathione peroxidase (GPx) levels in the liver homogenate were determined using a glutathione peroxidase assay kit (Cat #ab102530, Abcam, Cambridge, MA, USA). In this procedure, GPx reduces the probe cumene hydroperoxide while oxidizing GSH to GSSG. The generated GSSG is reduced to GSH with consumption of NADPH by glutathione reductase and the decrease of NADPH is proportional to GPx activity. The assay measures all types of glutathione-dependent peroxidases present in the sample. About 100 mg of frozen liver tissue was homogenized in 400 µl of ice-cold 50 mM Tris-HCl buffer (pH 8) containing 1 mM EDTA, and 1% Triton X-100. It was centrifuged at 10 000 *g* for 15 min at 4°C. About 25 µl of clear supernatant in a 96-well microplate was made up to 50 µl with assay buffer. It was mixed with 40 µl of reaction mix (containing assay buffer, NADPH, glutathione reductase and glutathione), and incubated at room temperature for 15 min. Then 10 µl cumene hydroperoxide solution was added, mixed well and read immediately at 340 nm on a microplate reader (FLUOstar Omega, BMG Labtech, Cary, NC, USA). It was allowed to stand for 5 min at room temperature and read again at 340 nm. One unit of GPx is defined as the amount of enzyme that will catalyze the oxidation of 1.0 µmol of NADPH to $NADP^+$ under the condition of the assay per minute at 25°C. Glutathione peroxidase activity in the liver tissue is presented as nmoles of NADPH oxidized/min/mg protein.

Determination of selenium in serum and liver

Selenium content in serum and liver samples was determined by ICP-MS after acid digestion of the sample and hydride generation of the selenium with sodium borohydride (Buckley et al., 1992). In ICP-MS, inductively coupled plasma acts as the ion source for the mass spectrometer. Inductively coupled plasma (ICP) is an electrodeless argon plasma formed at atmospheric pressure by

means of induction heating caused by a radio frequency electromagnetic field. The sample solutions were sprayed into the ICP with a nebulizer. Because of the high temperature of the plasma, dissolved solids are vaporized, atomized and ionized. Selenium ions were extracted into the mass spectrometer by means of differential pumping through a sampler and skimmer. Mass analysis was done by a quadrupole mass analyzer and the ions were detected by a channel electron multiplier. Based on the counts of selenium in known standards, the amount of selenium present in the unknown samples was determined.

Acid digestion and extraction of selenium from serum

Acid digestion for selenium was performed in a 25 ml extremely clean glass beaker with a cover glass. A hot plate was used for heating and the whole process was carried out inside a fume hood. All the acids used were analytical grade and were further purified by sub-boiling distillation in a quartz apparatus. For digestion, 0.5 ml of serum was treated with 0.5 ml concentrated HNO_3 and heated at 120–130°C for approximately 10 min. It was cooled and added 0.5 ml of quartz-distilled concentrated perchloric acid (70%) and heated for about 5–10 min until copious white fumes of perchloric acid was evolved at about 200°C. The process continued until the solution became clear and colorless. It was cooled and 0.5 ml of concentrated H_2SO_4 was added and heated at 280–300°C for 15 min. The use of higher temperature of 300°C was required for the complete decomposition and destruction of metalloenzymes to release selenium and to remove perchloric acid. The sample did not allow charring to prevent loss of selenium by evaporation. The sample was cooled, 1.0 ml of concentrated HCl was added, and heated at 110°C for 10–15 min in order to reduce the selenate to selenite. Whenever perchloric acid is added, selenite is easily oxidized to selenate (Watkinson, 1966). Selenate will not form hydrides efficiently like selenite. Finally, 1.25 ml of concentrated HCl was added followed by the addition of an internal standard, germanium, at a final concentration of 10 ng/ml of sample. An internal standard is required to take care of the instrumental drift during the operation. The sample was made up to 5.0 ml with deionized penta-distilled water (PDW) to obtain a final acid concentration of 3 M and 10-fold dilution of serum.

Acid digestion and extraction of selenium from the liver tissue

Exactly 100 mg wet liver tissue was weighed and dried in redistilled acetone. It was predigested with 2 ml of redistilled concentrated nitric acid in a very clean beaker with a cover glass at 110–120°C until it turned pale yellow. After cooling down to ambient temperature, 2 ml of quartz-distilled concentrated $HClO_4$ (70%) was added and digested at about 180°C until it became a clear and colorless solution. It was cooled and made up to 10 ml with PDW to obtain a final concentration of 10 mg of original liver tissue/ml. Two blanks were similarly treated and incorporated in the assay. Exactly 2 ml of the liver extract (digested with perchloric acid, 10 mg/ml) was treated with 0.5 ml of concentrated H_2SO_4 and followed the procedure as in serum. Finally, an internal standard was added and made up to 5.0 ml with deionized PDW to obtain a final concentration of 3 M acid and a liver extract of 4 mg/ml.

Standard and sample preparations

As ICP-MS is a very sensitive method for the determination of selenium, all possible measures were taken to avoid any chance of contamination at every processing and handling step. The standard solution was prepared and diluted in Corning 50 ml screw capped polypropylene centrifuge tubes (Corning, NY, USA). Prior to the standard preparation, every tube was rinsed with PDW 3 times. After the third rinsing, a prerun was carried out for selenium after the appropriate instrumental settings and made sure that all tubes used are free of selenium contamination. Selenium standard was prepared by dissolving 2.19 g specpure sodium selenite (Johnson Matthey Fine Chemicals, Cambridge, UK) in 100 ml of pentadistilled and deionized (18 MΩ) water. To obtain 1000 ppm (1 mg/ml) selenium, it was made up to 1 l with quartz distilled, diluted hydrochloric acid and the acidity was maintained as 1 N. The serum and liver samples were diluted in screw capped polypropylene tubes (Corning, NY, USA). Before dilution, all tubes were tested for any contamination of selenium. Eppendorf micropipette tips were rinsed with specpure *n*-heptane prior to use.

Hydride generation of selenium

As the detection limit of selenium is relatively poor in the direct solution nebulization method, the hydride generation technique has been adopted for a better analytical sensitivity in the determination of selenium by ICP-MS (Vijayalakshmi et al., 1992). In this technique, aqueous sample solutions are treated with a strong reducing agent after acidification to generate the volatile covalent hydride of the selenium. The hydride is then swept out of the generation vessel into the argon plasma torch of the ICP-MS where ionization takes place and the ions are analyzed and quantified by the mass spectrometer. In the present method, sodium borohydride ($NaBH_4$) was used as the reducing agent for the production of the hydrides (Nakahara, 1983).

$$NaBH_4 + 3H_2O + HCl \rightarrow H_3BO_3 + NaCl + 8H^{\cdot} \xrightarrow{Se4+} H_2Se + H_2 \text{ (excess)}$$

The $NaBH_4$ solution was freshly prepared and stabilized by alkalization with sodium hydroxide. For hydride generation, the selenium must be present as selenite in 3 M HCl which gives optimum results. The sample solutions (both serum and liver) and the sodium borohydride solution (2% sodium borohydride in 0.1 M sodium hydroxide) were introduced into the mixing chamber by a two-channel Gilson peristaltic pump (Gilson, Middleton, WI, USA) at the flow rate of 1.0 ml/min. The mixing chamber was connected to the nebulizer through tygon tubing to facilitate free passage of the hydrides. The volatile hydrogen selenides and the hydrogen gas produced in the mixing chamber were swept into the nebulizer successfully under their own pressure. Thus, selenium hydrides were continuously introduced into the ICP-MS (Vijayalakshmi et al., 1992).

Estimation of selenium

Selenium content in the samples was estimated after the introduction of selenium hydrides formed in the mixing chamber into the

argon plasma, where it was ionized and the ions were detected by a pulse counting channel electron multiplier as counts. All measurements were carried out using a Perkin-Elmer SCIEX^{R} ELAN™ 250 ICP-MS (Amherst, NY, USA). The argon flow was adjusted to 12 l/min for coolant and 1.4 l/min as an auxiliary. The sampling depth was 23 mm. The nebulizer argon flow was adjusted to 1.2 l/min. The readings were recorded in sequential mode with a measurement time of 0.5 s and with three measurements per peak. Sample measurements were repeated for 10 times and the mean value was taken. For serum, a calibration curve was constructed with 5–40 ng/ml selenium and for liver it was in the range of 1–5 ng/ml. The standard dilutions were prepared with distilled hydrochloric acid and the final acid concentration was adjusted to 3 M for the purpose of hydride generation.

Recovery of selenium in reference samples employing the ICP-MS method

In order to validate and evaluate the technique for the determination of selenium in biological samples, the rate of recovery of selenium has been studied after adding known concentrations of selenium to both serum samples and liver extract. In the case of serum, two known concentrations of selenium, 500 ng and 1 µg were added to 1 ml serum and mixed well. Six sets were prepared in both cases. In the case of liver, 50 ng and 100 ng selenium was added to 100 mg of liver extract in six sets of each. The same samples were incorporated in the assay without the addition of known amount of selenium. All the samples were treated in the same manner as described above for the determination of selenium in serum and liver tissue employing ICP-MS with hydride generation technique.

Statistical analysis

The mean and standard deviation were calculated for the data. The results were statistically evaluated using one-way analysis of variance. The control mean values were compared with the experimental mean values on days 7, 14, and 21 using the least significant difference method. Pearson's correlation coefficient was used to evaluate the linear relationship between decreased levels of glutathione and glutathione peroxidase activity and the correlation between reduced glutathione peroxidase and decreased selenium levels in the liver tissue.

Acknowledgments: The author is thankful to Dr. C. K. Mathews, Director, Chemical Group, Indira Gandhi Center for Atomic Research (IGCAR), Kalpakkam, Tamil Nadu, India for his permission to use the Perkin-Elmer SCIEX ELAN Inductively Coupled Plasma-Mass Spectrometer for the measurement of selenium. The technical assistance of Dr. Lisa George and Ms. S. Vijayalakshmi, Chemical Group, IGCAR, Kalpakkam is gratefully acknowledged. This work was supported by the Indian Council of Medical Research (Funder Id: 10.13039/501100001411), New Delhi, India, by grant no. 3/1/2/3/(9201540)/92-NCD-III to the author.

Conflicts of interest statement: The author does not have any conflicts of interest to declare in connection with this article.

References

Alegre, F., Pelegrin, P., and Feldstein, A.E. (2017). Inflammasomes in liver fibrosis. Semin. Liver Dis. *37*, 119–127.

Boosalis, M.G. (2008). The role of selenium in chronic disease. Nutr. Clin. Pract. *23*, 152–160.

Brenneisen, P., Steinbrenner, H., and Sies, H. (2005). Selenium, oxidative stress, and health aspects. Mol. Asp. Med. *26*, 256–267.

Brigelius-Flohé, R. and Maiorino, M. (2013). Glutathione peroxidases. Biochim. Biophys. Acta *1830*, 3289–3303.

Buckley, W.T., Budac, J.J., Godfrey, D.V., and Koenig, K.M. (1992). Determination of selenium by inductively coupled plasma mass spectrometry utilizing a new hydride generation sample introduction system. Anal. Chem. *64*, 724–729.

Burk, R.F., Early, D.S., Hill, K.E., Palmer, I.S., and Boeglin, M.E. (1998). Plasma selenium in patients with cirrhosis. Hepatology *27*, 794–798.

Casaril, M., Stanzial, A.M., Gabrielli, G.B., Capra, F., Zenari, L., Galassini, S., Moschini, G., Liu, N.Q., and Corrocher, R. (1989). Serum selenium in liver cirrhosis: correlation with markers of fibrosis. Clin. Chim. Acta *182*, 221–227.

Dworkin, B.M., Rosenthal, W.S., Stahl, R.E., and Panesar, N.K. (1988). Decreased hepatic selenium content in alcoholic cirrhosis. Dig. Dis. Sci. *33*, 1213–1217.

George, J. (2003). Ascorbic acid concentrations in dimethylnitrosamine-induced hepatic fibrosis in rats. Clin. Chim. Acta *335*, 39–47.

George, J. (2008). Elevated serum beta-glucuronidase reflects hepatic lysosomal fragility following toxic liver injury in rats. Biochem. Cell Biol. *86*, 235–243.

George, J. and Chandrakasan, G. (1996). Molecular characteristics of dimethylnitrosamine induced fibrotic liver collagen. Biochim. Biophys. Acta *1292*, 215–222.

George, J., Rao, K.R., Stern, R., and Chandrakasan, G. (2001). Dimethylnitrosamine-induced liver injury in rats: the early deposition of collagen. Toxicology *156*, 129–138.

George, J., Tsutsumi, M., and Tsuchishima, M. (2017). MMP-13 deletion decreases profibrogenic molecules and attenuates *N*-nitrosodimethylamine induced liver injury and fibrosis in mice. J. Cell. Mol. Med. *21*, 3821–3835.

Gheita, T.A. and Kenawy, S.A. (2014). Measurement of malondialdehyde, glutathione, and glutathione peroxidase in SLE patients. Methods Mol. Biol. *1134*, 193–199.

González-Reimers, E., Galindo-Martín, L., Santolaria-Fernández, F., Sánchez-Pérez, M.J., Alvisa-Negrín, J., García-Valdecasas-Campelo, E., González-Pérez, J.M., and Martín-González, M.C. (2008). Prognostic value of serum selenium levels in alcoholics. Biol. Trace Elem. Res. *125*, 22–29.

Gutiérrez, R., Alvarado, J.L., Presno, M., Pérez-Veyna, O., Serrano, C.J., and Yahuaca, P. (2010). Oxidative stress modulation by *Rosmarinus officinalis* in CCl_4-induced liver cirrhosis. Phytother. Res. *24*, 595–601.

Jamall, I.S., Finelli, V.N., and Que Hee, S.S. (1981). A simple method to determine nanogram levels of 4-hydroxyproline in biological tissues. Anal. Biochem. *112*, 70–75.

Khan, N., Jeong, I.S., Hwang, I.M., Kim, J.S., Choi, S.H., Nho, E.Y., Choi, J.Y., Park, K.S., and Kim, K.S. (2014). Analysis of minor and trace elements in milk and yogurts by inductively coupled plasma-mass spectrometry (ICP-MS). Food Chem. *147*, 220–224.

Korpela, H., Kumpulainen, J., Luoma, P.V., Arranto, A.J., and Sotaniemi, E.A. (1985). Decreased serum selenium in alcoholics as related to liver structure and function. Am. J. Clin. Nutr. *42*, 147–151.

Laclaustra, M., Navas-Acien, A., Stranges, S., Ordovas, J.M., and Guallar, E. (2009). Serum selenium concentrations and hypertension in the US Population. Circ. Cardiovasc. Qual. Outcomes *2*, 369–376.

Lin, X., Chen, Y., Lv, S., Tan, S., Zhang, S., Huang, R., Zhuo, L., Liang, S., Lu, Z., and Huang, Q. (2015). Gypsophila elegans isoorientin attenuates CCl_4-induced hepatic fibrosis in rats via modulation of NF-κB and TGF-β1/Smad signaling pathways. Int. Immunopharmacol. *28*, 305–312.

Liu, R.M. and Gaston Pravia, K.A. (2010). Oxidative stress and glutathione in TGF-β-mediated fibrogenesis. Free Radic. Biol. Med. *48*, 1–15.

Lu, C.W., Chang, H.H., Yang, K.C., Kuo, C.S., Lee, L.T., and Huang, K.C. (2016). High serum selenium levels are associated with increased risk for diabetes mellitus independent of central obesity and insulin resistance. BMJ Open Diabetes Res. Care *4*, e000253.

Lubos, E., Loscalzo, J., and Handy, D.E. (2011). Glutathione peroxidase-1 in health and disease: from molecular mechanisms to therapeutic opportunities. Antioxid. Redox Signal. *15*, 1957–1997.

Massadeh, A., Gharibeh, A., Omari, K., Al-Momani, I., Alomary, A., Tumah, H., and Hayajneh, W. (2010). Simultaneous determination of Cd, Pb, Cu, Zn, and Se in human blood of jordanian smokers by ICP-OES. Biol. Trace Elem. Res. *133*, 1–11.

Mormone, E., George, J., and Nieto, N. (2011). Molecular pathogenesis of hepatic fibrosis and current therapeutic approaches. Chem. Biol. Interact. *193*, 225–231.

Nakahara, T. (1983). Applications of hydride generation techniques in atomic absorption, atomic fluorescence and plasma atomic emission spectroscopy. Prog. Anal. At. Spectrosc. *6*, 163–223.

Ojeda, M.L., Carreras, O., Sobrino, P., Murillo, M.L., and Nogales, F. (2017). Biological implications of selenium in adolescent rats exposed to binge drinking: oxidative, immunologic and apoptotic balance. Toxicol. Appl. Pharmacol. *329*, 165–172.

Pemberton, P.W., Smith, A., and Warnes, T.W. (2005). Non-invasive monitoring of oxidant stress in alcoholic liver disease. Scand. J. Gastroenterol. *40*, 1102–1108.

Petrovski, B.E., Pataki, V., Jenei, T., Adány, R., and Vokó, Z. (2012). Selenium levels in men with liver disease in Hungary. J. Trace Elem. Med. Biol. *26*, 31–35.

Prystupa, A., Kiciński, P., Luchowska-Kocot, D., Błażewicz, A., Niedziałek, J., Mizerski, G., Jojczuk, M., Ochal, A., Sak, J.J., and Załuska, W. (2017). Association between serum selenium concentrations and levels of proinflammatory and profibrotic cytokines-interleukin-6 and growth differentiation factor-15, in patients with alcoholic liver cirrhosis. Int. J. Environ. Res. Public Health *14*, E437.

Ribas, V., García-Ruiz, C., and Fernández-Checa, J.C. (2014). Glutathione and mitochondria. Front. Pharmacol. *5*, 151.

Richter, K. and Kietzmann, T. (2016). Reactive oxygen species and fibrosis: further evidence of a significant liaison. Cell Tissue Res. *365*, 591–605.

Rua, R.M., Ojeda, M.L., Nogales, F., Rubio, J.M., Romero-Gómez, M., Funuyet, J., Murillo, M.L., and Carreras, O. (2014). Serum selenium levels and oxidative balance as differential markers in hepatic damage caused by alcohol. Life Sci. *94*, 158–163.

Sánchez-Valle, V., Chávez-Tapia, N.C., Uribe, M., and Méndez-Sánchez, N. (2012). Role of oxidative stress and molecular changes in liver fibrosis: a review. Curr. Med. Chem. *19*, 4850–4860.

Schmidt-Arras, D. and Rose-John, S. (2016). IL-6 pathway in the liver: from physiopathology to therapy. J. Hepatol. *64*, 1403–1415.

Seki, E. and Brenner, D.A. (2015). Recent advancement of molecular mechanisms of liver fibrosis. J. Hepatobiliary Pancreat. Sci. *22*, 512–518.

Thuluvath, P.J. and Triger, D.R. (1992). Selenium in chronic liver disease. J. Hepatol. *14*, 176–182.

Tinggi, U. (2008). Selenium: its role as antioxidant in human health. Environ. Health Prev. Med. *13*, 102–108.

Valimaki, M.J., Harju, K.J., and Ylikahri, R.H. (1983). Decreased serum selenium in alcoholics – a consequence of liver dysfunction. Clin. Chim. Acta *130*, 291–296.

Vijayalakshmi, S., Prabhu, R.K., Mahalingam, T.R., and Mathews, C.K. (1992). A simple gas-liquid separator for continuous hydride introduction in ICP-MS. At. Spectrosc. *13*, 26–28.

Watkinson, J.H. (1966). Fluorometric determination of selenium in biological material with 2,3-diaminonaphthalene. Anal. Chem. *38*, 92–97.

Zhang, C.Y., Yuan, W.G., He, P., Lei, J.H., and Wang, C.X. (2016). Liver fibrosis and hepatic stellate cells: etiology, pathological hallmarks and therapeutic targets. World J. Gastroenterol. *22*, 10512–10522.